A Novel Control Method for Forced Commutated Cycloconverters Using Instantaneous Values of Input Line-to-Line Voltages

著者	石黒　章夫
journal or publication title	IEEE Transactions on Industrial Electronics
volume	38
number	3
page range	166-172
year	1991
URL	http://hdl.handle.net/10097/46524

doi: 10.1109/41.87583

A Novel Control Method for Forced Commutated Cycloconverters Using Instantaneous Values of Input Line-to-Line Voltages

Akio Ishiguro, Takeshi Furuhashi, *Member, IEEE* and Shigeru Okuma, *Member, IEEE*

***Abstract*—Forced commutated cycloconverters (PWM cycloconverters) have no energy storage components except for small ac filters for the elimination of switching ripples. Therefore, the PWM cycloconverters can be made compact and highly reliable compared with the conventional converter-inverter systems. The PWM cycloconverters, however, directly connected the input terminals to the output terminals by the switching devices. As a result, if the input source voltages are asymmetrical and/or contain harmonics, the influence of the distortions directly appear on the output terminals. This problem is a major obstacle to using PWM cycloconverters instead of the conventional converter-inverter systems.**

This paper presents a novel control method for PWM cycloconverters. By using this control method, sinusoidal input and output current waveforms and unity input displacement factor can be obtained. Moreover, the compensation of the asymmetrical and/or harmonic contaminated input source voltages is easily realized.

I. Introduction

In recent years, forced commutated cycloconverters (PWM cycloconverters) have been studied to eliminate the dc links of the conventional converter-inverter systems. The PWM cycloconverters need no energy storage components except for small ac filters for elimination of switching ripples. As the result, the PWM cycloconverters can be made compact and highly reliable. Various methods for generating the switching patterns for the PWM cycloconverters have been proposed [1]–[9]. These control methods can be classified into two types. One is an indirect frequency conversion method [2]–[6]. This control method is based on the control methods of the conventional converter and inverter. Namely, ac–dc and dc–ac conversion signals are generated separately, and then PWM patterns for direct ac–ac conversion are obtained by synthesizing these signals. However, the method generates higher and fractional harmonic components in the input and output waveforms. As the result, it is difficult to achieve a real-time control, reducing these harmonic components. The other is a direct frequency conversion method [7]–[9]. This control method regards the frequency conversion as a coordinate transformation. Therefore, the PWM patterns for ac–ac conversion are generated directly, and sinusoidal input and output current waveforms with controllable input displacement factor regardless of the load power factor are obtained. Moreover, we proposed a method to obtain input and output current waveforms with smaller ripples by changing the switching sequence and the maximum input-to-output voltage ratio [9].

The PWM cycloconverters directly connect the input terminals to the output terminals by the switching devices. As the result, if the input source voltages are asymmetrical and/or contain harmonics, the influence of the distortions directly appear on the output terminal. This problem is a major obstacle in the use of the PWM cycloconverters in place of the conventional converter-inverter systems. The control functions proposed in [7]–[9] need complex calculations to compensate the distortions of the input source voltages. We think this difficulty is due to the vague physical meaning of the control method.

An output voltage control method for switched-mode rectifiers proposed by Aoki *et al.* realized unity input displacement factor by using input line-to-line voltages whose durations in a sampling period are proportional to their magnitudes [10]. However, the method has not been formulated, and it seems to not be suitable for real-time control for the compensation of the distortions of the input source voltages.

In this paper, we propose a new control method with a clear physical meaning by introducing the principle in [10]. The proposed control method synthesizes the demands of the output voltages using the instantaneous values of the input line-to-line voltages in each sampling period. However, if we simply incorporate the principle [10] into the control method of the PWM cycloconverters, a high switching frequency and a narrow output voltage range result. Thus, we propose a two-phase-switching method instead of using three input line-to-line voltages to overcome these problems. By using this control method, the compensation of the asymmetrical and/or harmonic contaminated input source voltages is easily realized. Furthermore, we show the proposed control functions include the conventional ones [7]–[9] in the case where the input source voltages are symmetrical and the input displacement factor is unity. This new control method allows the input displacement factor to not be controllable but to be fixed to be approximately unity. Since unity input displace-

Manuscript received May 1, 1990; revised December 18, 1990.
The authors are with the Department of Electronic—Mechanical Engineering, Nagoya University, Nagoya, Japan.
IEEE Log Number 9144458.

0278-0046/91/0600-0166$01.00

ment factor is desirable for motor-drive use for the PWM cycloconverters, this constraint is not a new obstacle to be used in the field. Therefore, we consider that the proposed control method is more practical compared with the conventional ones.

Finally, feasibility of the proposed control method is verified by simulations and experiments.

II. Configuration of the PWM Cycloconverters

The main circuit of the PWM cycloconverter is shown in Fig. 1(a), which consists of nine self-turn-off bidirectional switches, input ac filters, and symmetrical three-phase loads with Y connection, v_{uo}, v_{vo}, v_{wo}, and v_u, v_v, v_w denote the input source voltages and input voltages after the input ac filters, respectively. i_{uo}, i_{vo}, i_{wo} and i_u, i_v, i_w denote the input source currents and input currents after the input ac filters, respectively. v_a, v_b, v_c denote the output voltages viewed from the neutral point N, and i_a, i_b, i_c denote the output currents. r and l denote the resistance and inductance of the filter inductance, respectively, and the input ac filters for elimination of switching ripples consist of l and the filter capacitor C.

Examples of the bidirectional switches are shown in Fig. 1(b).

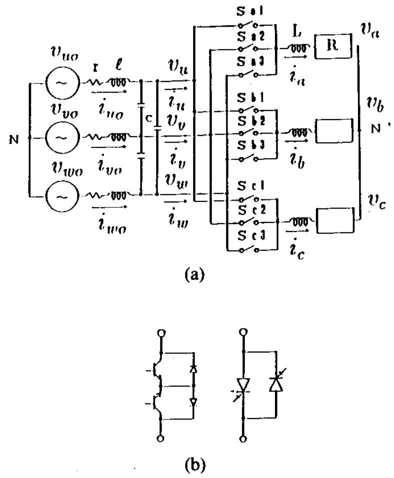

Fig. 1. PWM cycloconverter. (a) Main circuit; (b) bidirectional switching device.

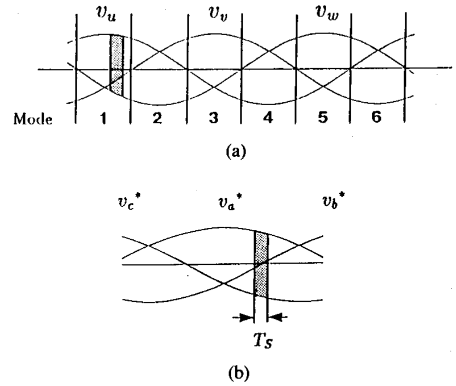

Fig. 2. Input and output voltage waveforms; (a) Input voltage waveforms; (b) output voltage waveforms.

III. Control Functions

A. Formulation of the Control Functions

Each switch of the PWM cycloconverter is controlled on and off depending on the demands of the output voltages v_a^*, v_b^*, v_c^* and the input voltages v_u, v_v, v_w.

For simplicity, the influence of the input ac filters is ignored, and the input voltages are symmetrical as the following:

$$\begin{pmatrix} v_u \\ v_v \\ v_w \end{pmatrix} = V_s \begin{pmatrix} \cos \omega_s t \\ \cos\left(\omega_s t - \dfrac{2\pi}{3}\right) \\ \cos\left(\omega_s t + \dfrac{2\pi}{3}\right) \end{pmatrix} \tag{1}$$

where V_s and ω_s denote the magnitude of the input source voltages and the input angular frequency, respectively. The waveforms of the input voltages v_u, v_v, v_w are shown in Fig. 2(a). We can devide one cycle of the input voltages v_u, v_v, v_w into six modes, as is shown in the figure.

In this paper, we propose the method that will realize the output voltages as shown in Fig. 2(b) by using three input line-to-line voltages v_{uv}, v_{vw}, v_{uw}. Assuming the values of the input voltages v_u, v_v, v_w and the output voltage demands v_a^*, v_b^*, v_c^* at a sampling period are given as in Fig. 2 (shaded portion), let us derive new control functions in mode 1.

The demands of the output line-to-line voltages v_{ab}^* and v_{ac}^* are synthesized by using the three input line-to-line voltages v_{uv}, v_{vw}, v_{uw} and zero voltage v_{uu} as follows:

$$v_{ab}^* = b_{12} \cdot v_{uv} + b_{23} \cdot v_{vw} + b_{13} \cdot v_{uw} + b_1 \cdot v_{uu} \tag{2}$$

$$v_{ac}^* = c_{12} \cdot v_{uv} + c_{23} \cdot v_{vw} + c_{13} \cdot v_{uw} + c_1 \cdot v_{uu} \tag{3}$$

where b_{12}, b_{23}, b_{13}, b_1, c_{12}, c_{23}, c_{13}, and c_1 denote the duty ratios of v_{uv}, v_{vw}, v_{uw}, and v_{uu} to be used in the sampling period, and the relationships of these variables are expressed as

$$b_{12} + b_{23} + b_{13} + b_1 = 1 \tag{4}$$

$$c_{12} + c_{23} + c_{13} + c_1 = 1 \tag{5}$$

where

$$0 \le b_{12} \le 1, 0 \le b_{23} \le 1, 0 \le b_{13} \le 1, 0 \le b_1 \le 1 \tag{6}$$

$$0 \le c_{12} \le 1, 0 \le c_{12} \le 1, 0 \le c_{13} \le 1, 0 \le c_1 \le 1. \tag{7}$$

In the periods of b_1 and c_1, the output voltages are zero. These periods make the adjustment of the mean values of the output voltages in the sampling period flexible. We determine the values of the duty ratios to be proportional to the magnitudes of the input line-to-line voltages. Namely, the on interval of a switch in each phase is proportional to the magnitude of the input voltage. Therefore, b_{12}, b_{23}, b_{13}, b_1, c_{12}, c_{23}, c_{13}, and c_1 are expressed as

$$b_{12} = \alpha \cdot v_{uv} \tag{8}$$

$$b_{23} = \alpha \cdot v_{vw} \tag{9}$$

$$b_{13} = \alpha \cdot v_{uw} \tag{10}$$

$$b_1 = 1 - b_{12} - b_{23} - b_{13} \tag{11}$$

$$c_{12} = \beta \cdot v_{uv} \tag{12}$$

$$c_{23} = \beta \cdot v_{vw} \tag{13}$$

$$c_{13} = \beta \cdot v_{uw} \tag{14}$$

$$c_1 = 1 - c_{12} - c_{23} - c_{13} \tag{15}$$

where α and β are coefficients corresponding to the voltage demands.

By substituting (8)–(15) into (2) and (3), we obtain the following equations:

$$v_{ab}^* = \alpha \cdot \left(v_{uv}^2 + v_{vw}^2 + v_{uw}^2\right) \tag{16}$$

$$v_{ac}^* = \beta \cdot \left(v_{uv}^2 + v_{vw}^2 + v_{uw}^2\right). \tag{17}$$

The values of b_{12}, b_{23}, b_{13}, c_{12}, c_{23}, and c_{13} are obtained by substituting (8)–(15) into (16) and (17) and by removing α and β as follows:

$$b_{12} = \frac{v_{uv} \cdot v_{ab}^*}{v_{uv}^2 + v_{vw}^2 + v_{uw}^2} \tag{18}$$

$$b_{23} = \frac{v_{vw} \cdot v_{ab}^*}{v_{uv}^2 + v_{vw}^2 + v_{uw}^2} \tag{19}$$

$$b_{13} = \frac{v_{uw} \cdot v_{ab}^*}{v_{uv}^2 + v_{vw}^2 + v_{uw}^2} \tag{20}$$

$$c_{12} = \frac{u_{uv} \cdot v_{ac}^*}{v_{uv}^2 + v_{vw}^2 + v_{uw}^2} \tag{21}$$

$$c_{23} = \frac{v_{vw} \cdot v_{ac}^*}{v_{uv}^2 + v_{vw}^2 + v_{uw}^2} \tag{22}$$

$$c_{13} = \frac{v_{uw} \cdot v_{ac}^*}{v_{uv}^2 + v_{vw}^2 + v_{uw}^2}. \tag{23}$$

Fig. 3 shows how to synthesize the output line-to-line voltages v_{ab}^*, v_{ac}^* in the sampling period.

This output voltage control method makes the input displacement factor unity in the case where the input voltages are sinusoidal and symmetrical. We use denotations of currents and voltages in Fig. 4. The output line-to-line voltages v_{ab} and v_{ac} are obtained by (2) and (3) in mode 1. Conversely, the input phase current i_{uv}, for example, is synthesized with the output currents i_{ab}, i_{ac}, and i_{bc} as

$$i_{uv} = b_{12} \cdot i_{ab} + c_{12} \cdot i_{ac} + \left(c_{12} - b_{12}\right) \cdot i_{bc}. \tag{24}$$

By (18) and (21), (24) is rewritten as

$$i_{uv} = \eta \cdot v_{uv} \tag{25}$$

where

$$\eta = \frac{v_{ab}^* \cdot i_{ab} + v_{ac}^* \cdot i_{ac} + v_{bc}^* \cdot i_{bc}}{v_{uv}^2 + v_{vw}^2 + v_{uw}^2}. \tag{26}$$

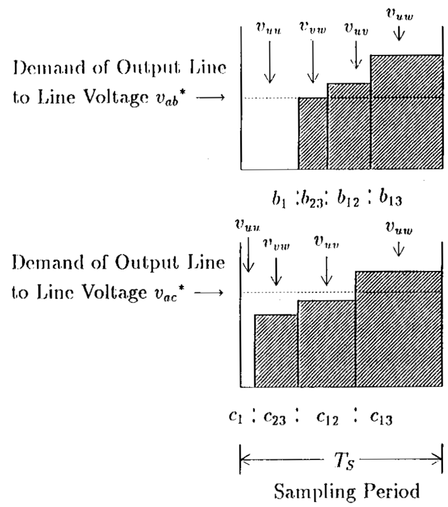

Fig. 3. Synthesizing method of output line-to-line voltages.

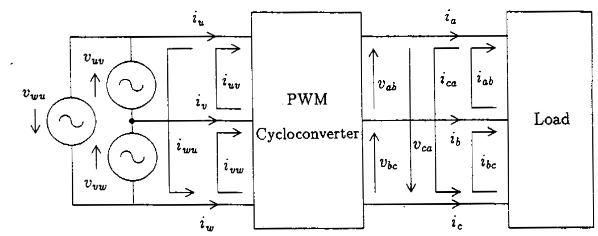

Fig. 4. Denotations of currents and voltages.

If the output voltages v_{ab}, v_{ac}, and v_{bc} are sinusoidal, the output currents i_{ab}, i_{ac}, and i_{bc} are also sinusoidal. When the input source voltages are sinusoidal and symmetrical, the coefficient η in (25) is constant. The input phase current i_{uv} is in phase with the input line-to-line voltage v_{uv}. It can also be proved that i_{vw} and i_{wu} are in phase with v_{vw} and v_{wu}, respectively. The input-to-output voltage ratio $A(\equiv \max V_{ab} / \max V_{uv})$ is derived from (6) and (7) and (18)–(23) as

$$A = 0.75. \tag{27}$$

The switching frequency of the PWM cycloconverter is determined by the switching terms in each sampling period. The switching times are dependent on the switching sequence. In the case of Fig. 3, the minimum switching times are realized by outputting the input voltages like this: $v_{uu} \rightarrow v_{uv} \rightarrow v_{uw} \rightarrow v_{vw} \rightarrow v_{uu}$. The total switching times in this sampling period is ten.

B. Improvement of the Control Functions

In the previous section, we formulated the control functions that use all the three input line-to-line voltages. We introduce the following two-phase-switching method, which realizes lower switching frequency and broader output voltage range than the method in the previous section does. Since u-phase voltage is the maximum during mode 1, as shown in Fig. 2(a), the switch S_{a1} is to be always connected to the A

phase, whereas the voltage v_a^* is the maximum of the output voltage demands. Thus, during this mode, the switches S_{b1}–S_{b3} and S_{c1}–S_{c3} are controlled to meet the output voltage demands v_{ab}^* and v_{ac}^*, respectively. During this mode, available input line-to-line voltages are v_{uv} and v_{uw}. Voltage v_{vw} is obtained as

$$v_{vw} = -(v_{uv} - v_{uw}). \tag{28}$$

The following equations are obtained by substituting (28) into (2) and (3):

$$v_{ab}^* = (b_{12} - b_{23}) \cdot v_{uv} + (b_{23} + b_{13}) \cdot v_{uw} \tag{29}$$

$$= b_1 \cdot v_{uu} + b_2 \cdot v_{uv} + b_3 \cdot v_{uw} \tag{30}$$

$$v_{ac}^* = (c_{12} - c_{23}) \cdot v_{uv} + (c_{23} + c_{13}) \cdot v_{uw} \tag{31}$$

$$= c_1 \cdot v_{uu} + c_2 \cdot v_{uv} + c_3 \cdot v_{uw} \tag{32}$$

where

$$b_1 + b_2 + b_3 = 1 \tag{33}$$

$$c_1 + c_2 + c_3 = 1. \tag{34}$$

The new variables b_1–c_3 correspond to the duty ratios of the switches S_{b1}–S_{c3} in the sampling period, respectively. b_1 and c_1 denote periods of zero output voltage for adjusting the mean values of output voltages in the sampling period. Fig. 5 shows how to synthesize the output line-to-line voltages v_{ab}^*, v_{ac}^* in a sampling period. The variables of b_1, b_2, b_3, c_1, c_2, and c_3 are the proposed control functions. When we use the switching sequence that outputs the input voltages as $v_{uu} \to v_{uv} \to v_{uw} \to v_{uu}$, the total switching times of this new method in a sampling period is six.

We can derive the control functions b_2, b_3, c_2, and c_3 from (18)–(23) and (29)–(32) as

$$b_2 = \frac{(v_{uv} - v_{vw}) \cdot v_{ab}^*}{v_{uv}^2 + v_{vw}^2 + v_{wu}^2} \tag{35}$$

$$b_3 = \frac{(v_{vw} - v_{wu}) \cdot v_{ab}^*}{v_{uv}^2 + v_{vw}^2 + v_{wu}^2} \tag{36}$$

$$c_2 = \frac{(v_{uv} - v_{vw}) \cdot v_{ac}^*}{v_{uv}^2 + v_{vw}^2 + v_{wu}^2} \tag{37}$$

$$c_3 = \frac{(v_{vw} - v_{wu}) \cdot v_{ac}^*}{v_{uv}^2 + v_{vw}^2 + v_{wu}^2}. \tag{38}$$

The control functions in other modes are obtained in the same way as in mode 1. For example, during mode 2, since w phase voltage is the minimum, the switch S_{c3} is turned on to connect the w phase to the C phase, where voltage v_c^* is the minimum as shown in Fig. 2(b). Thus, the demands of the output line-to-line voltages v_{ac}^*, v_{bc}^* are synthesized by the switches S_{a1}–S_{a3} and S_{b1}–S_{b3}, respectively. The control functions a_1–a_3 and b_1–b_3 corresponding to the switches S_{a1}–S_{a3} and S_{b1}–S_{b3} are derived, respectively.

The input-to-output voltage ratio using the improved control functions can be derived from the following constraints:

$$0 \le b_2 + b_3 \le 1 \tag{39}$$

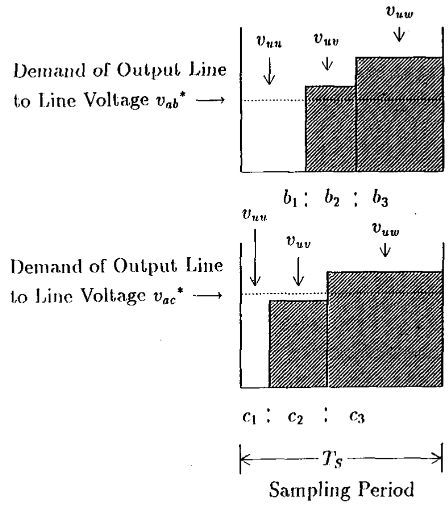

Fig. 5. Synthesizing method of output line-to-line voltages using two-phase switching method.

$$0 \le c_2 + c_3 \le 1. \tag{40}$$

From (39) and (40) and (35)–(38), we obtain the input-to-output voltage ratio as

$$A = \frac{\sqrt{3}}{2} (= 0.866). \tag{41}$$

The two-phase switching method realizes such improvements [9] as the increase of the input-to-output voltage ratio and the reduction of the harmonic distortion of the input and output waveforms by changing the switching sequence. In the case of symmetrical input source voltages, the denominators of the proposed control functions expressed by (35)–(38) become constant. Furthermore, we can use the following relations:

$$\frac{v_{uv} - v_{vw}}{3} = -v_{vo} \tag{42}$$

$$\frac{v_{vw} - v_{wu}}{3} = -v_{wo}. \tag{43}$$

The proposed control functions are rewritten as

$$b_2 = -k \cdot v_{vo} \cdot v_{ab}^* \tag{44}$$

$$b_3 = -k \cdot v_{wo} \cdot v_{ab}^* \tag{45}$$

$$c_2 = -k \cdot v_{vo} \cdot v_{ac}^* \tag{46}$$

$$c_3 = -k \cdot v_{wo} \cdot v_{ac}^* \tag{47}$$

where k denotes a coefficient.

Equations (44)–(47) show that the proposed control functions coincide with the conventional ones [9] and with the control principles [7], [8] in the case of unity input displacement factor.

For simplicity of explanation, the above derivation of the proposed control functions are explained on the assumption that the input source voltages are symmetrical, but no constraint on the input source voltages is introduced in the derivation. Assuming that $v_{uv}^{\sim}$, $v_{vw}^{\sim}$, and $v_{uw}^{\sim}$ denote asymmetrical and/or harmonic contaminated input line-to-line voltages, the output line-to-line voltages v_{ab}^{*} during mode 1 are synthesized using (30) and (32) and (35)–(38) as

$$v_{ab} = \frac{\left(v_{uv}^{\sim} - v_{uw}^{\sim}\right) \cdot v_{uv}^{\sim} + \left(v_{uv}^{\sim} - v_{wu}^{\sim}\right) \cdot v_{uw}^{\sim}}{v_{uv}^{\sim 2} + v_{vw}^{\sim 2} + v_{wu}^{\sim 2}} \cdot v_{ab}^{*} \quad (48)$$

$$= v_{ab}^{*}. \quad (49)$$

The other output line-to-line voltage v_{ac} also coincides with the demand v_{ac}^{*} in the same way.

Therefore, if the source voltages are asymmetrical and/or contain harmonics, the control functions will be modified automatically. The compensation of the distorted input voltages is easily realized without extra calculations.

The actual switching patterns are generated by the single-edged modulation method, in which the control functions are sampled and held to be compared with a sawtooth wave during each sampling period T_S, which is shown in Fig. 6.

IV. Simulation and Experimental Results

A. Symmetrical Input Source Voltages

Fig. 7 shows the simulation result of the proposed control method in the case where the three-phase input source voltages are balanced with the magnitude $V_s = 100$ V, the input-to-output voltage ratio $v_{out}/v_{in} = 0.7$, the input frequency (60 Hz), the output frequency (30 Hz), and the sampling period $T_S = 260$ μs. The input source currents i_{uo}, i_{vo}, i_{wo} are obtained by eliminating switching ripples from the input currents i_u, i_v, i_w with the input ac filters. The output currents i_a, i_b, i_c and the input source currents i_{uo}, i_{vo}, i_{wo} are nearly sinusoidal. The input source currents i_{uo}, i_{vo}, i_{wo} are nearly in phase with the source voltages v_{uo}, v_{vo}, v_{wo}, respectively.

Fig. 8(a) shows the experimental results of the waveforms of the input source voltage v_{uo} and the input source current i_{uo}. The input current i_{uo} leads to the input source voltages v_{uo} due to the current into the input filter capacitor. Fig. 8(b) shows the waveform of the output current i_a. The input and output currents are nearly sinusoidal. These experimental waveforms are obtained by off-line calculation of the control functions. The parameters used for the simulations and the experiments are listed on Table I.

B. Asymmetrical Input Source Voltages

Fig. 9 shows the simulation results of the conventional control method [9] in the case of asymmetrical input source voltages expressed as

$$\begin{pmatrix} v_{uo} \\ v_{vo} \\ v_{wo} \end{pmatrix} = \begin{pmatrix} V_1 \cos \omega_s t \\ V_2 \cos\left(\omega_s t - \dfrac{2\pi}{3}\right) \\ V_3 \cos\left(\omega_s t + \dfrac{2\pi}{3}\right) \end{pmatrix} \quad (50)$$

where $V_1 : V_2 : V_3 = 1 : 1 : 0.9$.

From this figure, it is known that the output current

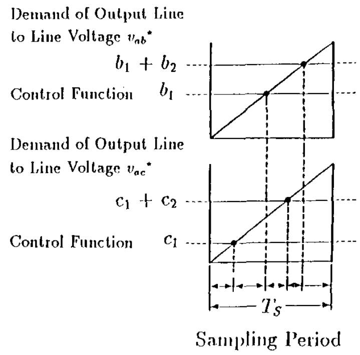

Fig. 6. Generating method of PWM patterns.

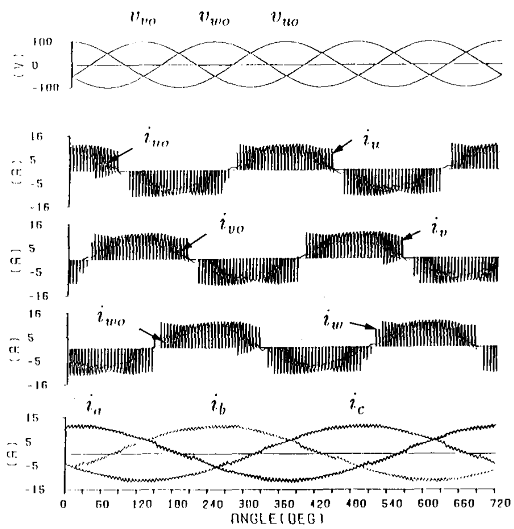

(Input: 60[Hz] Output: 30[Hz]
T_S = 260[μsec] V_{OUT}/V_{IN} = 0.7)

Fig. 7. Simulation result.

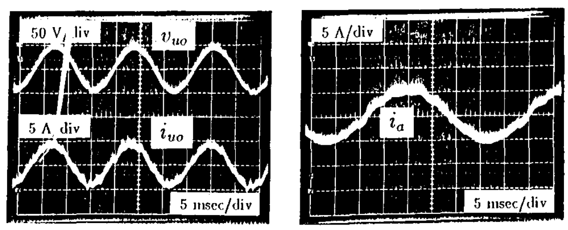

(Input: 60[Hz] Output: 30[Hz]
T_S = 260[μsec] V_{OUT}/V_{IN} = 0.7)

Fig. 8. Experimental result.

TABLE I
Parameters of the Circuit

INPUT ac FILTERS	$r = 0.50$ (Ω) $l = 0.60$ (mH) $C = 10.0$ (μF)
LOAD	$R = 6.0$ (Ω) $L = 3.5$ (mH)

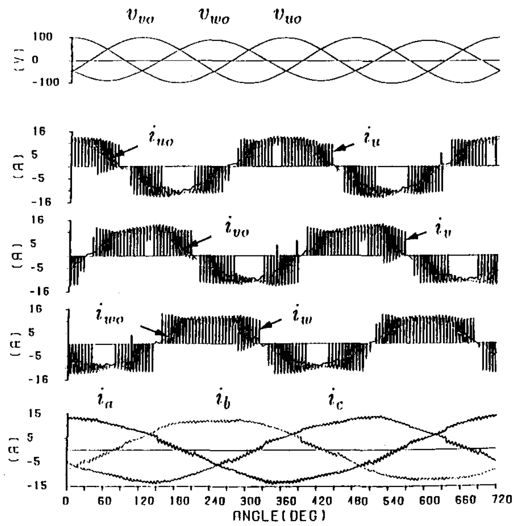

$$\begin{pmatrix} \textit{Input}: 60[Hz] & \textit{Output}: 30[Hz] \\ T_S = 260[\mu sec] & V_1 = 100[V] \\ V_2 = 100[V] & V_3 = 90[V] \end{pmatrix}$$

Fig. 9. Simulation result of the conventional method (asymmetrical input source voltages).

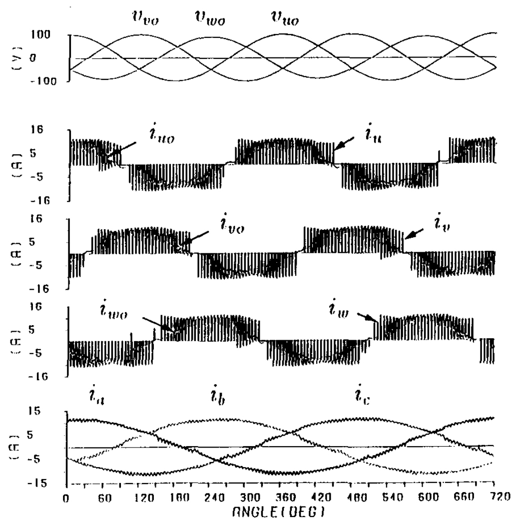

$$\begin{pmatrix} \textit{Input}: 60[Hz] & \textit{Output}: 30[Hz] \\ T_S = 260[\mu sec] & V_1 = 100[V] \\ V_2 = 100[V] & V_3 = 90[V] \end{pmatrix}$$

Fig. 10. Simulation result of the proposed method (asymmetrical input source voltages).

waveforms are distorted by the influence of the asymmetrical input source voltages.

Fig. 10 shows the waveforms of the proposed control method in the same conditions of those in Fig. 9. The output currents are nearly sinusoidal.

The mode detection of the input source voltages is done by using the output signal of the PLL circuit synchronized with the u-phase voltage v_u, and one cycle of the input source voltages are devided by 60° equally.

Figs. 10 and 11 show the experimental waveforms of the conventional and proposed control method, respectively. The conditions of the experiments are the same as those of the simulations.

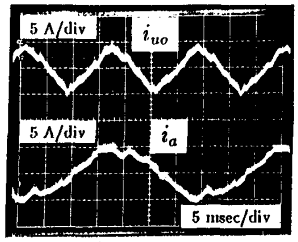

$$\begin{pmatrix} \textit{Input}: 60[Hz] & \textit{Output}: 30[Hz] \\ T_S = 260[\mu sec] & V_1 = 50[V] \\ V_2 = 50[V] & V_3 = 45[V] \end{pmatrix}$$

Fig. 11. Experimental result of the conventional method (asymmetrical input source voltages).

The output current waveform in Fig. 11 is distorted by the influence of the asymmetrical input source voltages, but the waveforms in Fig. 12 are nearly sinusoidal. The output currents in Figs. 11 and 12 contain higher harmonics. This is because the calculation of the control functions is carried out off line, and small ripples in the input source voltages are not compensated. These small ripples can be eliminated by on-line calculation of the proposed control functions. The waveforms of Figs. 11 and 12 almost coincide with the corresponding waveforms in Figs. 9 and 10, respectively. From these figures, the compensation is achieved by using the proposed control method.

C. Harmonic Contaminated Input Source Voltages

Figs. 13 and 14 show the simulation results using the conventional and proposed control methods, respectively. Harmonic contaminated input source voltages are expressed as

$$\begin{pmatrix} v_{uo} \\ v_{vo} \\ v_{wo} \end{pmatrix} = V_s \begin{pmatrix} \cos \omega_s t + \frac{1}{10} \cos 5\omega_s t \\ \cos\left(\omega_s t - \frac{2\pi}{3}\right) + \frac{1}{10} \cos 5\left(\omega_s t - \frac{2\pi}{3}\right) \\ \cos\left(\omega_s t + \frac{2\pi}{3}\right) + \frac{1}{10} \cos 5\left(\omega_s t + \frac{2\pi}{3}\right) \end{pmatrix}. \tag{51}$$

From these figures, the distortions of the input source voltages do not affect the output currents by using the proposed control method.

V. Conclusions

A novel PWM control method for the forced commutated cycloconverters is proposed. The results are as follows:

1) The control functions with a clear physical meaning are obtained using the input line-to-line voltages.

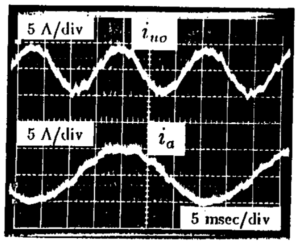

(Input: 60[Hz] Output: 30[Hz]
T_S = 260[μsec] V_1 = 50[V]
V_2 = 50[V] V_3 = 45[V])

Fig. 12. Experimental result of the proposed method (asymmetrical input source voltages).

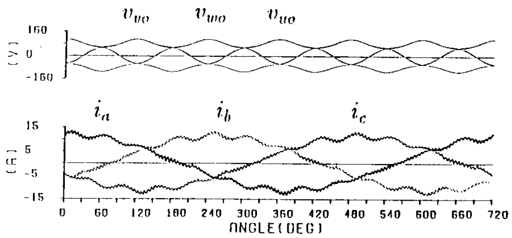

(Input: 60[Hz] Output: 30[Hz]
T_S = 260[μsec])

Fig. 13. Simulation result of the conventional method (with harmonics).

2) By introducing the two-phase switching method, reduction of the switching frequency and increase of the input-to-output voltage ratio are realized. The proposed control functions include the conventional ones in the case where the input displacement factor is unity.
3) The compensation for asynmetrical and/or harmonic contaminated input source voltages is realized.
4) Feasibility of the proposed control method is conformed by simulations and experiments.

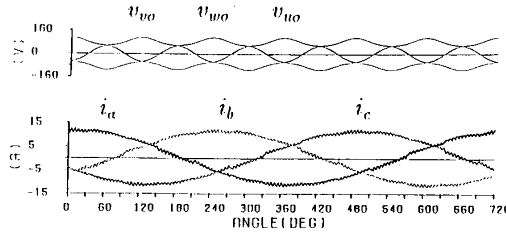

(Input: 60[Hz] Output: 30[Hz]
T_S = 260[μsec])

Fig. 14. Simulation result of the proposed method (with harmonics).

References

[1] T. Ohnishi *et al.*, "A novel PWM technique for three phase inverter/converter, in *Proc. IPEC* (Tokyo), 1983, p. 384.

[2] P. D. Ziogas *et al.*, "PWM control techniques for rectifier filter minimization, *IEEE Trans. Industry Applications*, vol. IA-21, p. 1206, 1985.

[3] —, "Optimum system design of a three-phase rectifier-inverter type of frequency changer, *IEEE Trans. Industry Applications*, vol. IA-21, p. 1215, 1985.

[4] A. R. Daniel *et al.*, "Application of power transistor to polyphase regenerative power converters," *Proc. Inst. Elec. Eng.*, vol. 125, p. 643, 1978.

[5] P. D. Ziogas *et al.*, "Some improved forced commutated cycloconverter structures," *IEEE Trans. Industry Applications*, vol. IA-21, p. 1242, 1985.

[6] P. D. Ziogas *et al.*, "Analysis and design of forced commutated cycloconverter structures with improved transfer characteristics, in *Proc. IEEE PESC*, 1985, p. 610.

[7] M. Venturini, "A new sine wave in sine wave out conversion technique eliminates reactive elements," *Proc. Powercon 7*, 1980, pp. E3-1–E3-15.

[8] A. Alesina and M. Venturini, "A analysis and design of optimum-amplitude nine-switch direct ac-ac converters, *IEEE Trans. Power Elec.*, vol. PE-4, pp. 101, 1980.

[9] A. Ishiguro *et al.*, "A new method of PWM control for forced commutated cycloconverters using microprocessors," *IEEE IAS Ann. Mtg.*, 1988, p. 712.

[10] T. Aoki *et al.*, "A new switched-mode rectifier with sinusoidal input current waveforms," in *Proc. IPEC* (Tokyo), 1990, p. 755.